International Journal of Women's Health

Dovepress
Taylor & Francis Group

Open Access Full Text Article

ORIGINAL RESEARCH

Single-Cell Transcriptomic Analysis Highlights the Impact of NFKB2-Mediated MIF-CD44 Signaling Axis in Endometrioid Endometrial Cancer

Lu Zhang[1,2,*], Mengjie Yang[1,2,*], Quan Zhang[2], Yiqian Zhang[1,2], Qiyuan Li[2], Qionghua Chen[1,2]

[1]Laboratory of Research and Diagnosis of Gynecological Diseases of Xiamen City, Clinical Medical Research Center for Obstetrics and Gynecology Diseases of Fujian Province, Department of Obstetrics and Gynecology, the First Affiliated Hospital of Xiamen University, School of Medicine, Xiamen University, Xiamen, People's Republic of China; [2]National Institute for Data Science in Health and Medicine, Xiamen University, Xiamen, People's Republic of China

*These authors contributed equally to this work

Correspondence: Qiyuan Li, National Institute for Data Science in Health and Medicine, Xiamen University, No. 4221-121, Xiang'an South Road, Xiang'an District, Xiamen, Fujian, People's Republic of China, Email qiyuan.li@xmu.edu.cn; Qionghua Chen, Department of Obstetrics and Gynecology, the First Affiliated Hospital of Xiamen University, 24 Bailu Road, Siming District, Xiamen, Fujian, Email cqhua616@126.com

Background: The tumor microenvironment (TME) is a complex network driving endometrioid endometrial cancer (EC) progression. Previous analyses of the EC TME were often limited by a lack of detailed cellular annotations. Integrating single-cell RNA sequencing (scRNA-seq) data offers a comprehensive approach to reconstruct the TME, aiming to uncover novel mechanisms and therapeutic targets.

Methods: We integrated public scRNA-seq data from 15 EC and 5 normal endometrium samples. Through detailed cell annotation, we performed comprehensive bioinformatic analyses, including pseudotime trajectories, copy number variation, and cell communication, to investigate mechanisms of EC development.

Results: We identified nine cell types and characterized subpopulations of epithelial, macrophage, lymphocyte, and stromal fibroblast cells. The SOX9+LGR5- epithelial subtype showed elevated malignancy and NFKB pathway enrichment. The M2_like2 macrophage subtype played a critical role, engaging in robust MIF-(CD74+CD44) mediated communication with SOX9+LGR5- cells. Experimental validation confirmed MIF co-expression with E-cadherin in EC tissues. Furthermore, the transcription factor NFKB2 was found to mediate MIF's effect on the CD44 receptor in malignant epithelial cells. A pericyte-to-fibroblast transition in stromal cells may also support tumor growth, while an increase in CD8 exhausted/Treg cells and a decrease in cytotoxic CD8 cells suggest potential immune evasion.

Conclusion: Our single-cell analysis details the EC TME landscape, revealing robust communication between M2_like2 macrophages and SOX9+LGR5- epithelial cells. We highlight a key mechanism where NFKB2 mediates MIF's pro-tumorigenic effects via the CD44 receptor, offering new insights into EC progression and potential therapeutic targets.

Keywords: endometrial cancer, single-cell RNA sequencing, tumor microenvironment, cell communication

Introduction

Endometrial cancer (EC) comprises a group of epithelial malignancies that manifest in the endometrium. It ranks as the second most prevalent among malignant tumors affecting the female reproductive system in China and is the most common in developed countries.[1] The tumor microenvironment (TME) denotes the localized internal milieu consisting of tumor cells, stromal cells, and the extracellular matrix, collectively fostering tumor initiation and progression.[2] Various elements within this microenvironment interconnect to create a complex network that propels the malignant transformation and evolution of endometrial epithelial cells.[3] Single-cell RNA sequencing (scRNA-seq) technology facilitates unbiased, reproducible, high-resolution, and high-throughput transcriptional analysis of individual cells, rendering it an

Received: 29 April 2025
Accepted: 5 September 2025
Published: 26 September 2025

indispensable tool for investigating the tumor microenvironment, tumor pathogenesis, and tumor diagnosis and treatment.[3,4] Previous research has delineated the characteristics of endometrial epithelial cells in EC, outlining a cellular landscape of the tumor immune microenvironment.[5] Through exploration of cell-cell and cell-matrix interactions within the TME, researchers have identified close interactions between malignant cells in EC and immune cells and tumor-associated fibroblasts, leading to the discovery of potential therapeutic targets.[6] Another study elucidated the roles of B cells and tertiary lymphoid structures in the immune response to EC and identified prognostic biomarkers.[7] A study utilized single-cell transcriptomic sequencing analysis to identify various cell types within normal endometrium, atypical hyperplastic endometrium, and endometrioid carcinoma, revealing the dynamic evolution of cell subpopulations during the progression from normal endometrium to endometrioid carcinoma.[8] Another research, combined with spatial transcriptomic analysis, unveiled the role of tumor-associated macrophages in EC patients' response to anti-PD-1 therapy, particularly focusing on immunotherapy sensitivity.[9] While previous single-cell studies have provided valuable insights, their scope has often been limited. These analyses have predominantly focused on specific cell subpopulations, or presented cellular annotations with varying granularity across studies. This fragmented approach hinders a holistic understanding of the complex intercellular crosstalk across the entire TME. In contrast, our study directly addresses this gap by integrating multiple scRNA-seq datasets. This strategy allows us to construct a unified, high-resolution atlas of the EC TME, enabling a comprehensive analysis of all major cell populations and their interactions within a single analytical framework.

Overall, in this study, we integrated 15 cases of endometrial cancer and 5 cases of normal data from public databases to restructure the endometrial cancer microenvironment. We provided detailed annotation of important subpopulations and compared our findings with other published studies. Furthermore, we discovered a strong communication between the macrophage subpopulation M2_like2 and the epithelial cell subpopulation SOX9+LGR5-. Experimental validation confirmed that MIF was co-expressed with the epithelial cell marker E-cadherin in EC tissues, with the transcription factor NFKB2 mediating MIF's effects on the CD44 receptor of SOX9+LGR5- epithelial cells.

Methods

Single-Cell RNA-Seq Data Preprocessing

We acquired publicly available data from databases published by Guo et al.[5] Ren et al[8] and Regner et al[10] encompassing 15 cases of endometrioid endometrial cancer and 5 cases of normal endometrial data (Appendix Table 1). To prepare files for subsequent RNA velocity analysis, we downloaded the raw data and processed the raw sequencing reads of human endometrial cells using the CellRanger software suite (10x Genomics Cell Ranger 4.0.0). We utilized the reference genome refdata-gex-GRCh38-2020-A and mapped the reads to the human genome (GRCh38/hg38), generating a unique molecular identifier (UMI) matrix.[11] The output data from CellRanger were loaded using the "Read10X" function in Seurat.[12] Each sample underwent individual filtering based on UMI counts and mitochondrial proportions as part of the quality control process (Appendix Table 1). Following quality filtering, we selected a total of 147,438 cells from 20 subjects for subsequent analysis.

Dimensionality Reduction, Clustering, and Annotation

Post-normalization, we identified highly variable genes using the FindVariableGenes function in Seurat. These genes were employed for principal component analysis (PCA).[13] Subsequently, we created a two-dimensional representation of the data using UMAP with the first 40 principal components (PCs). On the PCA-reduced expression data, we applied the FindClusters algorithm in Seurat to identify clusters at a resolution of 0.3. This algorithm calculated the neighborhood overlap between each cell and its nearest neighbors. The graph-based clustering results were visualized in the two-dimensional space using UMAP.[14] To mitigate batch effects, we conducted the harmony algorithm for batch correction before clustering analysis,[15] followed by applying FindNeighbors and FindCluster in Seurat to delineate cell subtypes. We assigned known biological cell types to the cell clusters via marker genes reported in the literature and differential expression analysis. The FindAllMarkers function in the Seurat package was utilized to analyze differences between

clusters. A gene was classified as a marker gene if it was expressed in at least 25% of the cells and had a minimum log-fold change threshold of 0.25.

Functional Enrichment Analysis

Gene set enrichment analysis was performed on differentially expressed genes using the Gene Ontology (BP, CC, and MF) and the Kyoto Encyclopedia of Genes and Genomes (KEGG) pathway database.[16] The ClusterProfiler R package was employed for GO and KEGG analyses.[17] GSEA displayed enriched gene sets for each gene's expression.[18] The Seurat built-in gene set scoring function AddModuleScore was utilized for scoring.[19]

Estimation of Copy Number Variations (CNVs)

We utilized the R package InferCNV (https://github.com/broadinstitute/inferCNV) to calculate CNVs from single-cell transcriptomic data of fifteen patients with endometrial cancer, using five samples from normal endometrial tissues as the reference. We identified somatic large-scale chromosomal CNVs for each gene (cutoff = 0.1). Subsequently, we generated a heatmap to visualize the CNV profiles of specific cell types and chromosomal segments. To assess CNV variations across different cell types, we centered the Hidden Markov Model predicted matrix around zero and computed the sum of squares to determine cell-based CNV levels.[20]

Pseudotime Analysis

We employed the Monocle 2.0 package (version 2.10.0) to analyze single-cell trajectories and infer the continuous process of cell differentiation.[21] Genes expressed in fewer than three cells were excluded. Library size normalization was executed using the "estimateSizeFactors" function, and the negative binomial dispersion for each gene was estimated using the "estimateDispersions" function. Genes with an average expression greater than 0.5 and a variance larger than the empirical dispersion (best-fit mean-dispersion trendline) were selected. We employed DDTree for the dimensionality reduction of the selected genes and subsequently constructed the trajectory using the "orderCells" function.

RNA Velocity Analysis

RNA velocity analysis estimated the change in RNA abundance over time by measuring the ratio of mRNA before and after splicing using standard single-cell sequencing data, which can be applied to study the dynamic differentiation of cell gene expression. RNA velocity analysis was conducted using the Python package scVelo to investigate cell type transitions.[22] Count matrices for unspliced (pre-mRNA) and spliced (mature mRNA) abundances were generated using the "velocyto" package from the BAM files obtained from CellRanger, with the latter serving as input for scVelo. Leveraging the dynamic model in scVelo, we projected the results back onto the UMAP generated by Seurat.

SCENIC Analysis

We performed SCENIC analysis using pyscenic (version 0.9.19) and the hg19-500bp-upstream-10species database with RcisTarget, GRNboost, and AUCell. The input matrix comprised the normalized expression matrix from Seurat. To compute the regulon activity scores (RAS) of cells, we utilized the pySCENIC Python package for SCENIC analysis.[23] Initially, we used GRNBoost2 to infer co-expression modules between TFs and candidate target genes. Subsequently, RcisTarget was employed to analyze the genes within each co-expression module to identify enriched motifs (defining TFs and their potential direct target genes as regulons). Finally, we evaluated the activity of each regulon in every cell using AUCell.

Cell Communication Analysis

We employed the CellChat tool[24] for quantitatively inferring cell-cell communication based on scRNA-seq data to determine intercellular communication. CellChat was utilized to elucidate critical cellular pathways involved in cell clustering. netVisual circles were used to depict the network of cell clusters relative to other cell clusters, whereas netVisual_bubble was employed to display interactions of ligand-receptor crosstalk between cell clusters.

TCGA Data Analysis

The Transcripts Per Kilobase per Million mapped reads (TPM) data and clinical parameters of Uterine Corpus Endometrial Carcinoma (TCGA-UCEC) was downloaded using the Bioconductor TCGAbiolinks package (version 2.10.5).[25] We included 409 samples with EC and 35 normal samples out of the 589 samples for downstream expression level comparison. To assess the expression and prognostic value of genes, samples were further divided into "low expression" and "high expression" groups based on the average gene expression level. Statistical analysis was performed using the R package "survival" (version 3.1.8). Survival curves were fitted using the survfit function, and differences between the high and low expression groups were tested using the survdiff test.

Cell Culture

All EC cells were purchased from the American Type Culture Collection (ATCC). Ishikawa and KLE cells were cultured in DMEM/F12 with 10% FBS, while AN3CA cells were maintained in EMEM with 10% FBS. HEC-1A cells were grown in McCoy's 5A medium supplemented with 100 mmol/L sodium pyruvate and 10% FBS. RL95-2 cells were cultured in DMEM/F12 with 0.005 mg/mL insulin and 10% FBS. All cells were incubated at 37°C with 5% CO2.

When cells reached 80% confluence, they were incubated overnight in serum-free medium, then treated with various concentrations of rhMIF (MCE, HY-P7387) (0, 5, 10, 15, 25, and 50 ng/mL) for 24 hours before being harvested for protein extraction.

Small Interfering RNA (siRNA) Transfection

All siRNAs, including the negative control siRNA (#1027281), were purchased from RiboBio, with the target sequences for NFKB2 being stB0003825A/B/C. Transfection was performed according to the manufacturer's protocols using Lipofectamine RNAiMAX (Invitrogen).

Western Blot

Western Blot analysis was performed as described in our previous work.[26] The information and dilution rates of antibodies in this study were NFKB2 (Proteintech, #10409-2-AP, 1:500), CD44 (Proteintech, #15675-1-AP, 1:2000), and GAPDH (Proteintech, #60004-1-Ig, 1:10,000).

Immunofluorescence

To assess the cellular localization of MIF protein in EC tissues, immunofluorescence was employed to label conserved markers. Tissue samples were fixed, dehydrated, and embedded following established protocols. The slides were then incubated overnight at 4°C with primary antibodies, including those against MIF (Proteintech, #20415-1-AP, 1:100) and E-cadherin (CST, #14472, 1:100). After three PBS washes, the slides were incubated with the appropriate fluorescent secondary antibodies at room temperature for 1 hour. Nuclei were stained with DAPI solution, and the results were observed and photographed using a fluorescence microscope (Olympus Corporation, Tokyo, Japan).

Statistical Analysis

Data were analyzed using GraphPad Prism software. For comparisons between two groups, statistical evaluation was conducted using a two-tailed Student''s s *t*-test. For categorical data, chi-square tests were used to compare groups. P-value < 0.05 was considered statistically significant.

Results

Single-cell Transcriptomic Profiling of Human Endometrial Cancer

After stringent filtering, a total of 147,438 single cells were retained for further bioinformatics analysis (Figure 1A). We performed PCA and UMAP to reduce dimensionality based on gene expression normalization. Subsequently, graph-based clustering was employed to classify cells into 16 clusters (Figure 1B), and specific marker genes were used to annotate these clusters, resulting in the identification of nine cell types: lymphocytes (marked by PTPRC, CCL5,

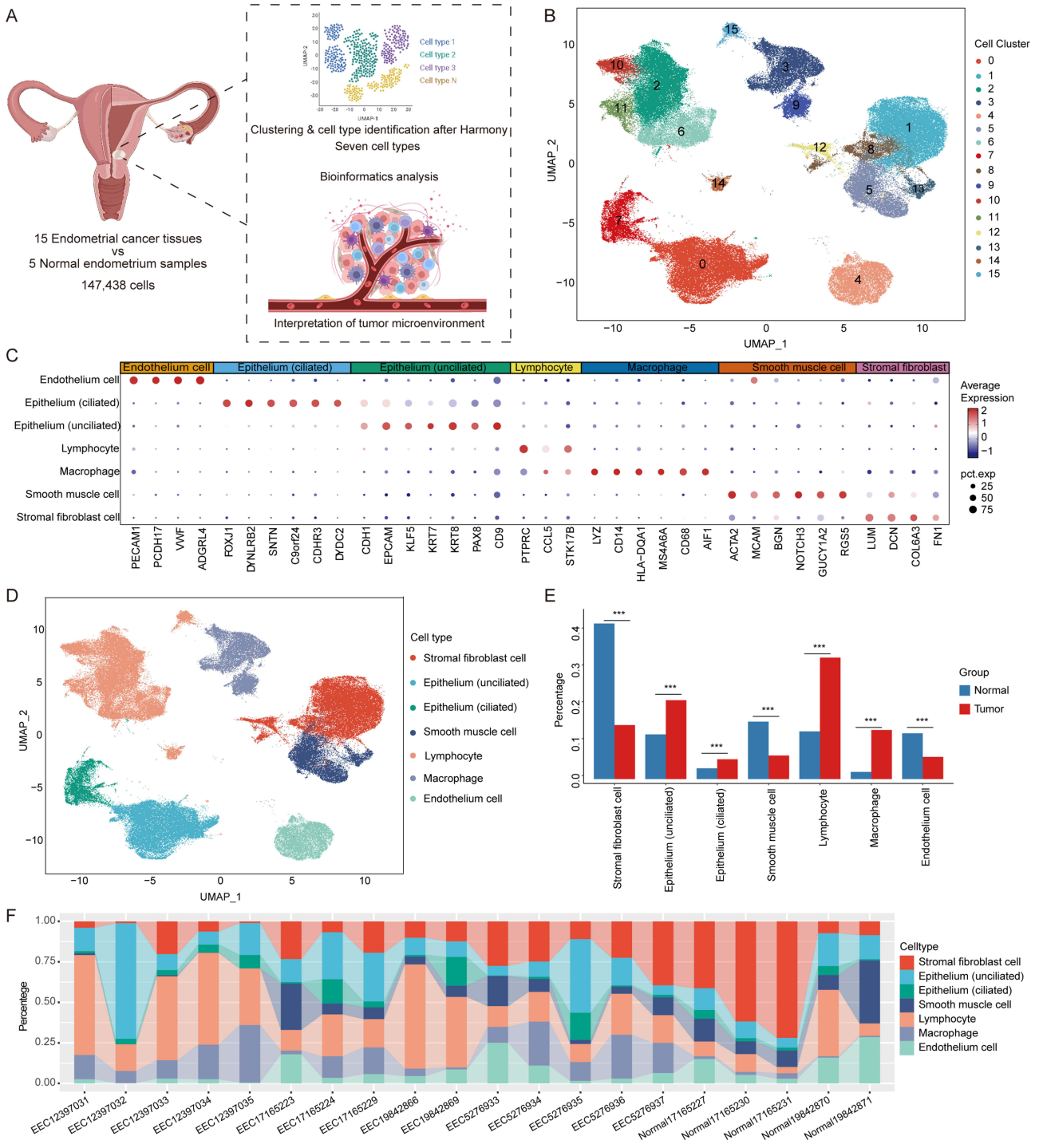

Figure 1 Provided a comprehensive overview of human endometrial cancer. (**A**) Illustrated the scRNA-seq analysis workflow. (**B**) Illustrated 16 cell clusters within 147,438 cells using UMAP plots. (**C**) Displayed marker genes for 7 distinct cell types through bubble plots. (**D**) Identified distinct cell types using marker genes. (**E**) Illustrated the proportion of cell types through bar plots based on statistical analysis. (**F**) Depicted the proportion of cell types in each sample using bar plots. Levels of significance were defined as *$p < 0.05$, **$p < 0.01$, and ***$p < 0.001$.

STK17B), macrophages (marked by LYZ, IL1B, CD14, HLA-DQA1, MS4A6A, CD68), stromal fibroblasts (marked by LUM, DCN, COL6A3, PDGFRB), smooth muscle cells (marked by ACTA2, MCAM, BGN, NOTCH3, RGS5), endothelial cells (marked by PECAM1, PCDH17, VWF, ADGRL4), ciliated epithelial cells (marked by FOXJ1, DYNLRB2, SNTN, C9orf24, CDHR3), and unciliated epithelial cells (marked by CDH1, EPCAM, KLF5, KRT7,

https://doi.org/10.2147/IJWH.S530666

KRT8, PAX8) (Figure 1C and D). The proportions of each cell type between different groups showed significant differences after statistical analysis (Figure 1E). Notably, significant differences were observed in the proportions of each cell type among different samples, indicating heterogeneity among tumors in endometrial cancer (Figure 1F).

Epithelial Cells in the Endometrial Microenvironment and Increase in the SOX9 +LGR5- Proportions

To gain a better understanding of the subtypes of epithelial cells, further analysis was conducted by performing re-clustering and dimensionality reduction analysis on epithelial cells from both normal tissue and tumor samples. The UMAP projection revealed that epithelial cells were divided into 9 clusters (Appendix Figure 1A). Using known markers obtained from published literature, the cell clusters were assigned to six epithelial subtypes (Figure 2A). Pre-ciliated cells and Ciliated cells showed high expression of the transcription factor FOXJ1, PGR, and PIFO, which are associated with active cilia and ciliogenesis. Ciliated-LGR5+ cells additionally displayed high expression of LGR5. Glandular secretory cells exhibited high expression of GPX3, SLC26A2, PODXL, CLDN10, and PAEP (Appendix Figure 1B). There was a significant increase in the proportion of SOX9+LGR5- cells within endometrial cancer tissues (Appendix Figure 1C). Additionally, a notable increase was observed within the ciliated cell population (Figure 2B).

Increase in CNVs in SOX9+LGR5- and Specific Programs Identified Through NMF Algorithm

Endometrial cancer originates from epithelial cells. Therefore, it can be assumed that tumor cells undergoing malignant transformation are present within the epithelial tissue. To distinguish the malignant status of cells, we calculated large-scale chromosomal CNVs for each cell type based on the average expression patterns of the genome. We found that the CNV levels in SOX9+LGR5- epithelial cells were significantly higher than those in other cell types. The heatmap revealed extensive amplifications or deletions in SOX9+LGR5- cells (Figure 2C). Considering that the proportion of SOX9+LGR5- cells exhibited the greatest variation among all epithelial cell subtypes, this study posits that this cluster played a crucial role in the development of endometrial cancer (Appendix Figure 1C and Appendix Table 2). Therefore, GSEA analysis was conducted to investigate its biological functions. The results showed that the upregulated genes in this cluster of cells in tumor samples mainly identified significant activation of the NFKB signaling pathway, indicating a malignant state (Figure 2D). Considering that various subtypes of epithelial cells in tumor tissues exhibited a certain degree of malignancy in the aforementioned results (Figure 2E), NMF analysis was performed on epithelial cells from tumor tissues. It revealed the clustering of malignant epithelial cells into six distinct programs (Figure 2F). It can be observed that epithelial cells may play specific roles in the regulation of cell adhesion, cell growth, cilium movement, RNA processing, and signal transduction, among other related functions (Figure 2G). In conclusion, malignant epithelial cells in endometrial cancer may exert different roles in tumor progression. In our study, we examined the metagenes within the programs and identified several genes, such as LCN2, which have been previously reported to be highly expressed in carcinogenic subgroups in studies conducted by Ren et al (Appendix Table 3). Additionally, genes like CD44 and CD74 were also identified. These findings serve as evidence of the applicability of this method in uncovering biological features and further understanding the gene characteristics of carcinogenic subgroups.

Trajectory Analysis Revealed the Lineage and Dynamics of Epithelial Cells

Monocle trajectory and RNA velocity analysis were performed on epithelial subtypes to establish their developmental trajectories. Pseudotime analysis revealed that different subtypes formed a relative developmental trajectory, starting from glandular secretory cells and gradually differentiating into SOX9+LGR5- and SOX9+LGR5+ cells, ultimately differentiating into ciliated cells (Figure 3A and Appendix Figure 2A). In SOX9+LGR5- cells, there was high expression of genes recognized in other literature as a cancerous subcluster marker (Appendix Figure 2B). These cells also exhibited high expression of markers associated with glandular epithelium, indicating that this cluster of cells is in a transitional state between the two, playing an important role in the occurrence and development of endometrial cancer. In the overall cells of the three clusters SOX9+LGR5+, SOX9+LGR5-, and Pre-ciliated, the proportions of spliced mRNA and

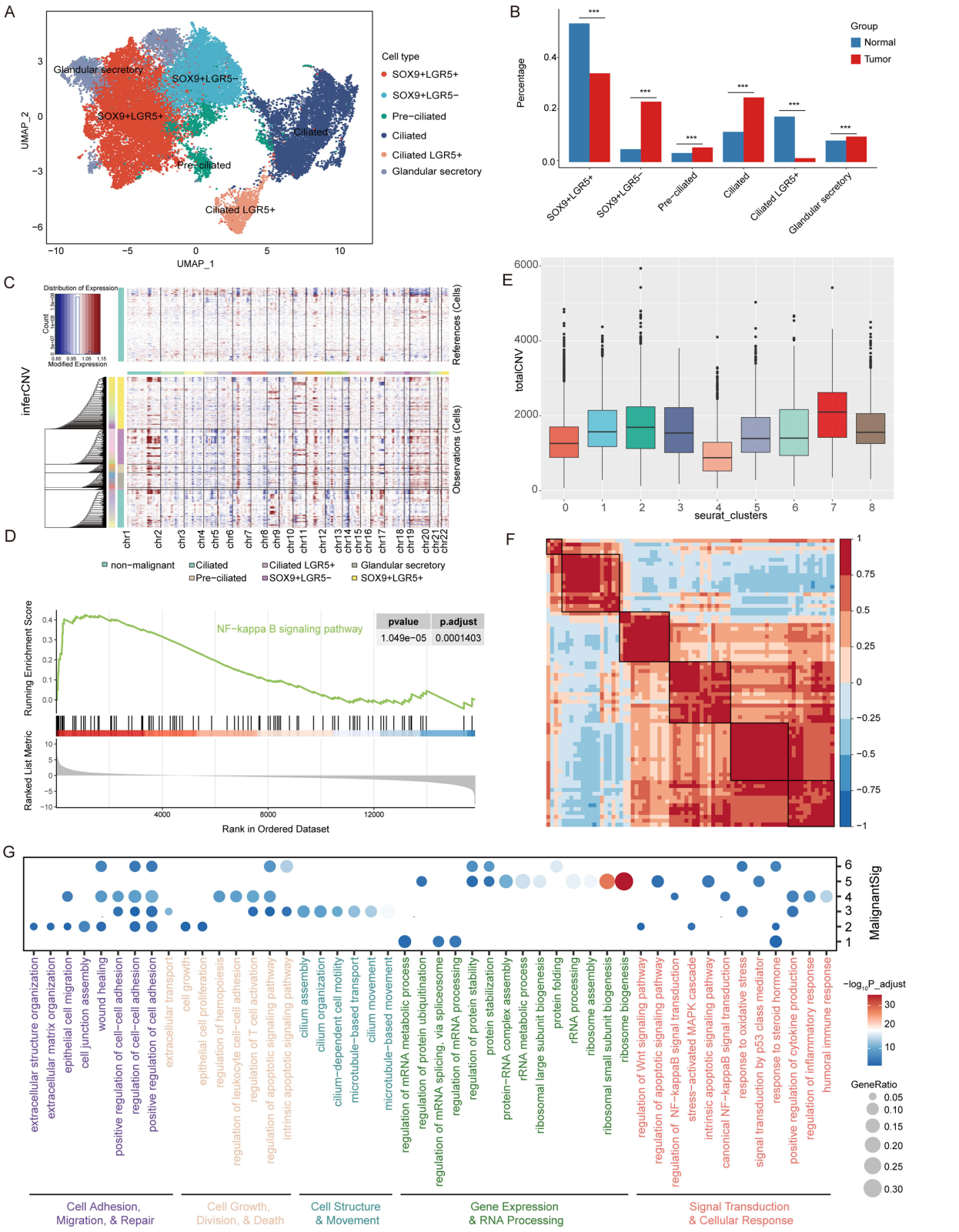

Figure 2 Examined the cell population landscapes of epithelial cells in the endometrial microenvironment. (**A**) UMAP projection revealed the division of epithelial cells into 9 clusters. (**B**) Noted significant changes in the proportion of epithelial cells in the normal and tumor groups. (**C**) Identified extensive amplifications or deletions in SOX9 +LGR5- cells through a heatmap. (**D**) Demonstrated a high degree of malignancy in 9 clusters through CNV scoring. (**E**) Identified significant activation of the NFKB signaling pathway in SOX9+LGR5- cells from tumor samples. (**F**) Revealed clustering of malignant epithelial cells into six distinct programs through NMF analysis. (**G**) Highlighted specific roles of epithelial cells in the regulation of cell adhesion, growth, cilium movement, RNA processing, and signal transduction. Levels of significance were defined as $*p < 0.05$, $**p < 0.01$, and $***p < 0.001$.

https://doi.org/10.2147/IJWH.S530666

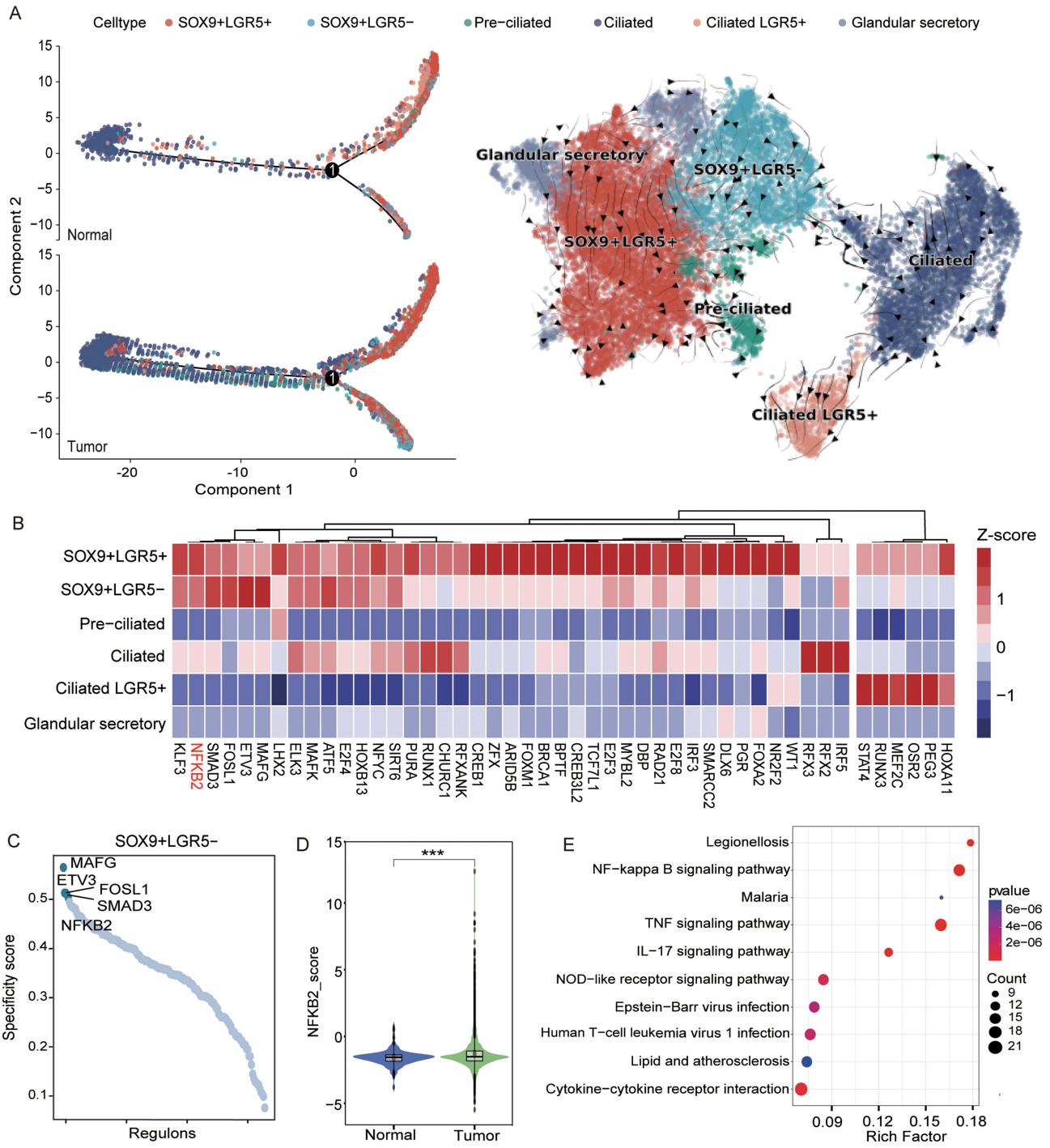

Figure 3 Established the trajectory lineage of epithelial cells and identified epithelial subtype-specific gene regulatory transcription. (**A**) Revealed a relative developmental trajectory formed by different subtypes through pseudotime analysis. (**B**) Identified the top five TFs with high activity specific to the SOX9+LGR5- subtype of endometrial cancer using the SCENIC algorithm. (**C**) Displayed the activity of the top five TFs within six epithelial cell subtypes through a heatmap. (**D**) Showed significantly enhanced activity of the NFKB2 transcription factor in endometrial cancer through functional enrichment scoring. (**E**) Revealed significant enrichment of NFKB signaling pathways in SOX9+LGR5- cells from tumor samples through GO functional enrichment analysis. Levels of significance were defined as $*p < 0.05$, $**p < 0.01$, and $***p < 0.001$.

unspliced mRNA were 53% and 46%, 55% and 44%, and 57% and 42%, respectively. Additionally, 1% represented ambiguous mRNA. Overall, the spliced mRNA was more abundant than unspliced mRNA in accordance with biological expectations (Appendix Figure 2C). It revealed a similar evolutionary trajectory, which could be clearly observed that glandular secretory cells differentiated towards SOX9+LGR5- and SOX9+LGR5+ directions. (Figure 3A).

Identification of Epithelial Subtype-Specific Gene Regulatory Transcription

We attempted to identify TFs to better understand the establishment and maintenance of epithelial subtypes in the endometrial cancer tumor microenvironment. To achieve this, we applied the SCENIC algorithm to identify the top five TFs with high activity specific to cell clusters within the epithelial subtypes of endometrial cancer (Figure 3B and C, Appendix Figure 2D). We observed distinct patterns of highly expressed TFs in epithelial cells. MAFG belongs to the MAF family, while FOSL1 belongs to the FOS family. Additionally, NFKB2, a member of the NFKB family of molecules involved in regulating immune and inflammatory responses, and SMAD3, a key member of the TGFB family, are also implicated. Through functional enrichment scoring using addModuleScore on the NFKB2 transcription factor and its target genes, it was observed that their activity was significantly enhanced in endometrial cancer (Figure 3D). GO functional enrichment analysis was conducted on the SOX9+LGR5- cells, revealing significant enrichment in common cancer-related pathways such as the NFKB and TNF signal pathways (Figure 3E).

Macrophages in the Endometrial Microenvironment and Increase of the M2-like2 Proportions

To delve deeper into macrophage subtypes and enhance comprehension, we conducted a re-clustering analysis of macrophages in both normal tissue and tumor samples. The UMAP projection unveiled the subdivision of macrophages into 14 clusters (Appendix Figure 3A and B). Subsequently, using established markers from the literature, we categorized the cell clusters into nine subtypes (Figure 4A and Appendix Figure 3C). Monocyte cells exhibited heightened expression of S100A12 and S100A9, while one of the M2-like macrophages, M2_like1, displayed increased expression of genes such as MAF, TNF, and the M2_like2 subtype specifically expressed genes like RAB13, DAB2, TXNIP, PDK4, and C1QC. M1_like1 macrophages showcased elevated expression of genes such as FCER1A, CD1C, CLER1A, and PLD4, whereas M1_like2 macrophages demonstrated heightened expression of genes like FYN, TENT5C, RORA, and ETS1. M_remodeling cells exhibited elevated expression of genes including TPM2, MYL9, ADIRF, and MGP. DCs cells demonstrated high expression of genes such as CCDC126, CLEC9A, and CPNE3. Mast cells displayed increased expression of genes like TPSAB1, CPA3, and MS4A2, while neutrophils exhibited high expression of CD24. An overall increase in the expression of M2_macrophages and a decrease in M1_macrophages were observed in endometrial cancer. Particularly, there was a notable rise in the proportion of M2_like2 within endometrial cancer tissues (Figure 4B).

Increase of CNVs in Myeloid Cells and Identification of Specific Programs Through NMF

The heatmap revealed extensive amplifications or deletions of M2_like2 cells in these cells (Figure 4C). Given the significant variation in the proportion of M2_like2 cells among all macrophage subtypes, this study suggested that this cluster played a pivotal role in the development of endometrial cancer (Appendix Table 4). Enrichment analysis indicated that the upregulated genes in M2_like2 of tumor samples primarily pointed towards a significant activation of the Oxidative phosphorylation signaling pathway, suggesting a state of high energy consumption (Figure 4D).

Considering that various subtypes of epithelial cells in tumor tissues exhibited a certain degree of malignancy in the aforementioned results (Figure 4E), NMF analysis was conducted on myeloid cells from tumor tissues, revealing the clustering of myeloid cells into six distinct programs (Figure 4F). It was evident that myeloid cells may have specific roles in inflammatory responses, fluid shear stress, atherosclerosis, NF-KB signaling pathway, and other related functions (Figure 4G). We scrutinized the metagenes within the programs and identified the presence of the previously recognized drug resistance gene MIF, as reported in studies by Hu et al (Appendix Table 5).

Trajectory Analysis Reveals the Lineage and Dynamics of Macrophages

Pseudotime analysis disclosed that different subtypes followed a relative developmental trajectory, commencing from monocyte cells, progressively differentiating into M1-like cells, polarizing into M2-like macrophages, and ultimately differentiating into M_remodeling cells, contributing to cellular remodeling functions. Macrophages were notably abundant in tumors and displayed a continuum of macrophage activation states. Compared to normal tissues, monocyte

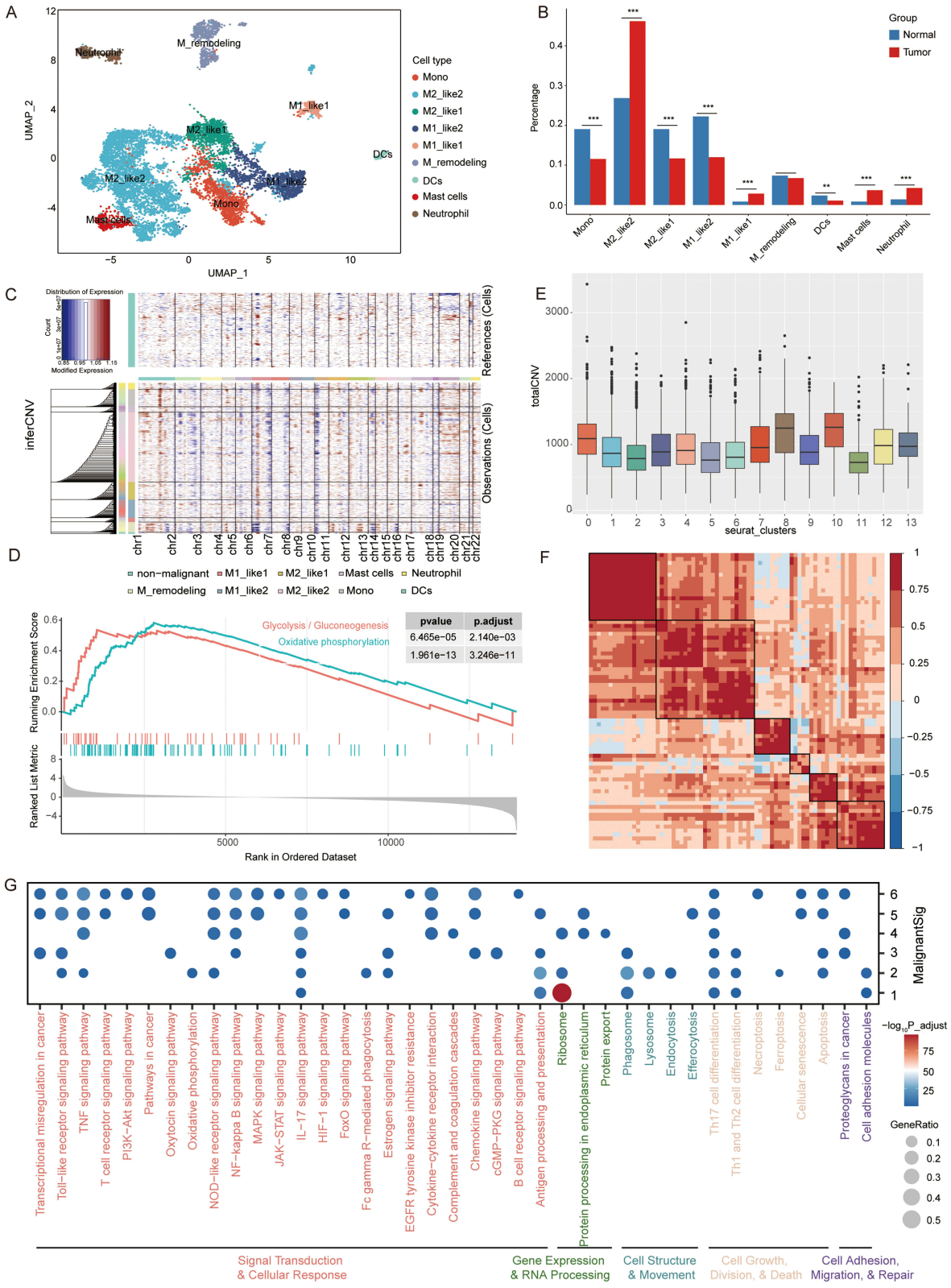

Figure 4 Examined the cell population landscapes of macrophages in the endometrial microenvironment. (**A**) The UMAP projection revealed macrophages divided into nine subtypes. (**B**) Significantly increased the proportion of M2_like2 within endometrial cancer tissues. (**C**) The heatmap revealed extensive amplifications or deletions in M2_like2 cells. (**D**) CNV scoring of macrophages demonstrated a high degree of malignancy in 14 clusters. (**E**) GO functional enrichment analysis revealed significant activation of the Oxidative phosphorylation signaling pathway in M2_like2 cells from tumor samples. (**F**) NMF analysis revealed clustering of malignant myeloid cells into six distinct programs. (**G**) Myeloid cells played specific roles in regulating the inflammatory response, fluid shear stress, atherosclerosis, and the NF-KB signaling pathway. Levels of significance were defined as $*p < 0.05$, $**p < 0.01$, and $***p < 0.001$.

differentiation into macrophages appeared to be less efficient, along with two subtypes of M2 macrophages, differentiated into M_remodeling cells (Figure 5A and Appendix Figure 3D). RNA velocity analysis showcased a similar evolutionary trajectory, supporting the ongoing process of macrophage differentiation. Specifically, monocyte cells initially differentiated into M1-like2 cells, gradually transitioning towards M2-like1 type. M2-like cells also underwent a transformation towards M2-like1 type (Figure 5B). Regarding the ratio of spliced to unspliced mRNA within cells, spliced mRNA was observed to be more abundant than unspliced mRNA (Appendix Figure 3E).

Identification of Myeloid Subtype-Specific Gene Regulatory Transcription

To better comprehend the establishment and maintenance of Myeloid subtypes, we proceeded to identify TFs using the SCENIC algorithm. This analysis aimed to identify the top five TFs with high activity specific to cell clusters within the Myeloid subtypes of the endometrial cancer tumor microenvironment (Figure 5C and D, Appendix Figure 4A). Distinct patterns of highly expressed TFs were observed in each subtype. For example, the M2-like2 subtype exhibited high activity of transcription factors such as CEBPA, STAT1, IRF9, MXI1, and MAX (Figure 5C).

Lymphocytes in the Endometrial Microenvironment

We conducted a re-clustering of lymphocytes to investigate the inherent heterogeneity of the immune microenvironment. The lymphocytes were categorized into 17 clusters, representing 12 cell types, including CD8 exhausted, CD4 naive, CD8 naive, CD4 cytotoxic, CD8 cytotoxic, Proliferation_T, NK cells, Treg, ILC3, B cells, plasma cells, and NKT (Figure 6A, Appendix Figure 5A and B). The exhausted cell type was characterized by PDCD1 and CD8A. Naive T cells were identified by CD3D and IL7R. Cytotoxic T cells were marked by GZMA and GZMB. Regulatory T cells were distinguished by FOXP3 and TNFRSF4. Proliferation_T cells were labeled with MKI67, PCNA, and STMN1. NK cell markers included NCAM1, NKG7, and FCGR3A, while NKT cell markers were FGFBP2 and CX3CR1. B cell markers were CD78B, MS4A1, and TCL1A. Plasma cells, a specialized type of B cells, were identified by MZB1 and SDC1 (Appendix Figure 5C). Analysis of cell subtype proportions revealed significant alterations in lymphocyte ratios in endometrial cancer tissue compared to the normal group, except for CD4 cytotoxic cells. Notably, Treg, CD4 naive, CD8 exhausted, CD8 cytotoxic, Proliferation_T, plasma cells, and B cells were markedly increased (Figure 6B).

Stromal Fibroblasts in the Endometrial Microenvironment

Intense stromal reactions are commonly observed in various malignant tumors such as cervical cancer and colorectal cancer. We re-clustered stromal fibroblasts and categorized them into 12 clusters, representing 9 cell types (Figure 6C, Appendix Figure 5D and E). eS exhibited elevated expression of genes such as COL1A1, COL3A1, and PCOLCE. Activated fibroblasts (Matrix FB) displayed specific gene expressions like LUM, DCN, and VCAN, while pericytes showed high expression of RGS5 and GJA4 genes. Myofibroblast markers were ACTA2, CNN1, and FAP. Fibro C7 cells exhibited high complement C7 and OGN expressions. MKI67+FB represented a proliferating cell cluster with elevated MKI67 and PCNA expression. Antigen-presenting fibroblasts (Ap FB) showcased high immune-related gene expressions such as CD74 and HLA-DRA. Lipid fibroblasts (Lip FB) displayed significant FAB1 and FABP4 expressions. Furthermore, there was a cluster of endo-like fibroblasts (Endo-like FB) with notable VWF, PECAM1, and other gene expressions (Appendix Figure 5F). The proportion of 9 different cell types within stromal fibroblasts showed a significant change between the two groups (Figure 6D). Pseudotime analysis unveiled a relative developmental trajectory where distinct subtypes progressed from eS to activated fibroblasts (Matrix FB), followed by differentiation into myofibroblasts and pericytes (Figure 6E, Appendix Figure 5G and H). In endometrial cancer tissue, pericytes underwent pericyte-fibroblast transition (PFT) to differentiate into terminal FBs, contributing to ECM deposition and possibly promoting tumor invasion and metastasis (Figure 6E, Appendix Figure 5G and H).

Cell Communication in the Endometrial Microenvironment and Experimental Validation

In endometrial cancer epithelial cells, SOX9+ cells displayed significant segmental amplifications or deletions, indicating a high level of malignancy. While current research on endometrial cancer focuses on myeloid cells at a preliminary

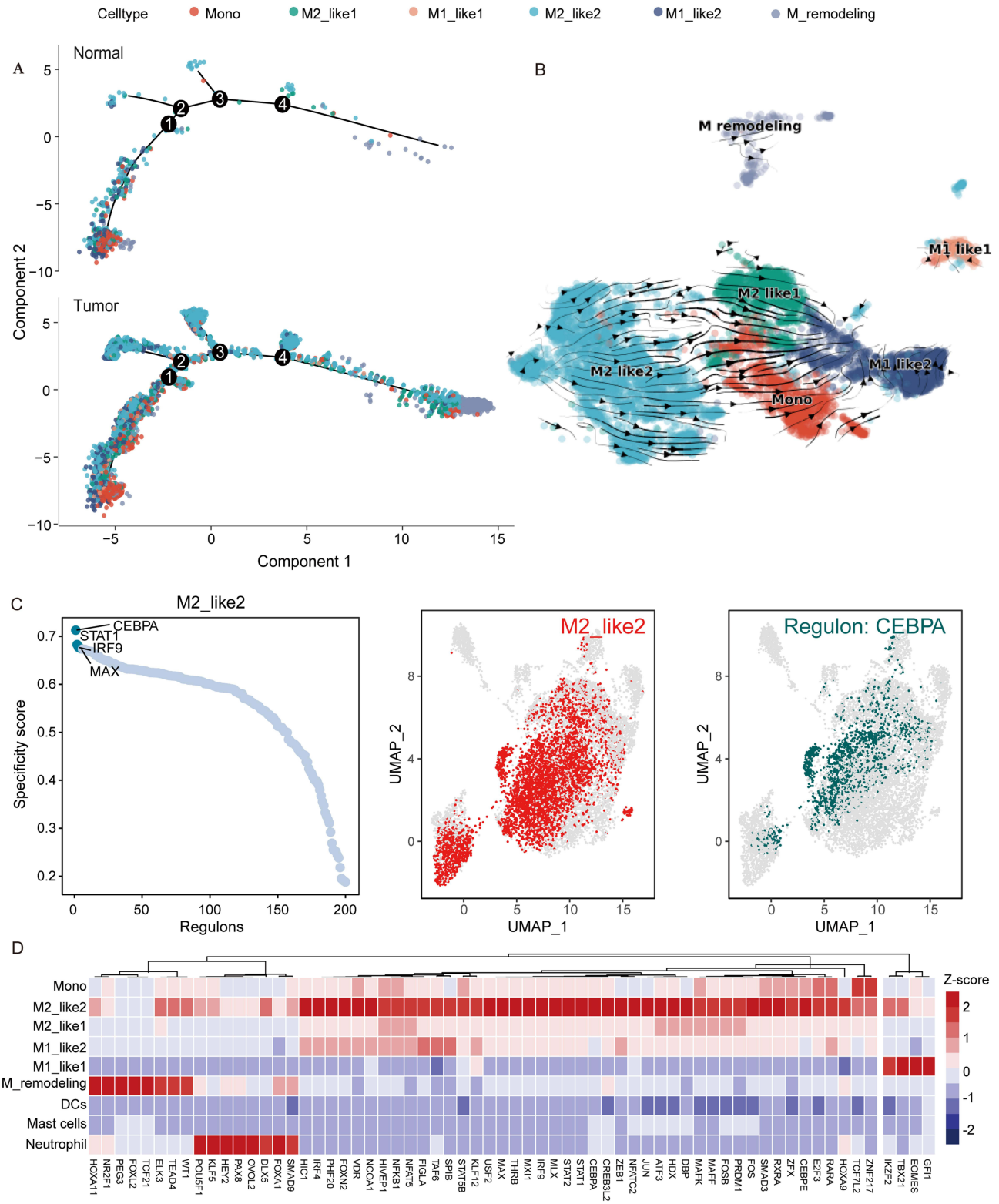

Figure 5 Established the trajectory lineage of myeloid cells and identified subtype-specific gene regulatory transcription. (**A**) Pseudotime analysis revealed different subtypes forming a relative developmental trajectory of myeloid cells. (**B**) RNA velocity analysis showcased different subtypes forming a relative developmental trajectory of myeloid cells. (**C**) Identified the top five TFs with high activity specific to M2_like2 in endometrial cancer using the SCENIC algorithm. (**D**) The heatmap displayed the activity of the top five TFs with high activity specific to nine myeloid subtypes.

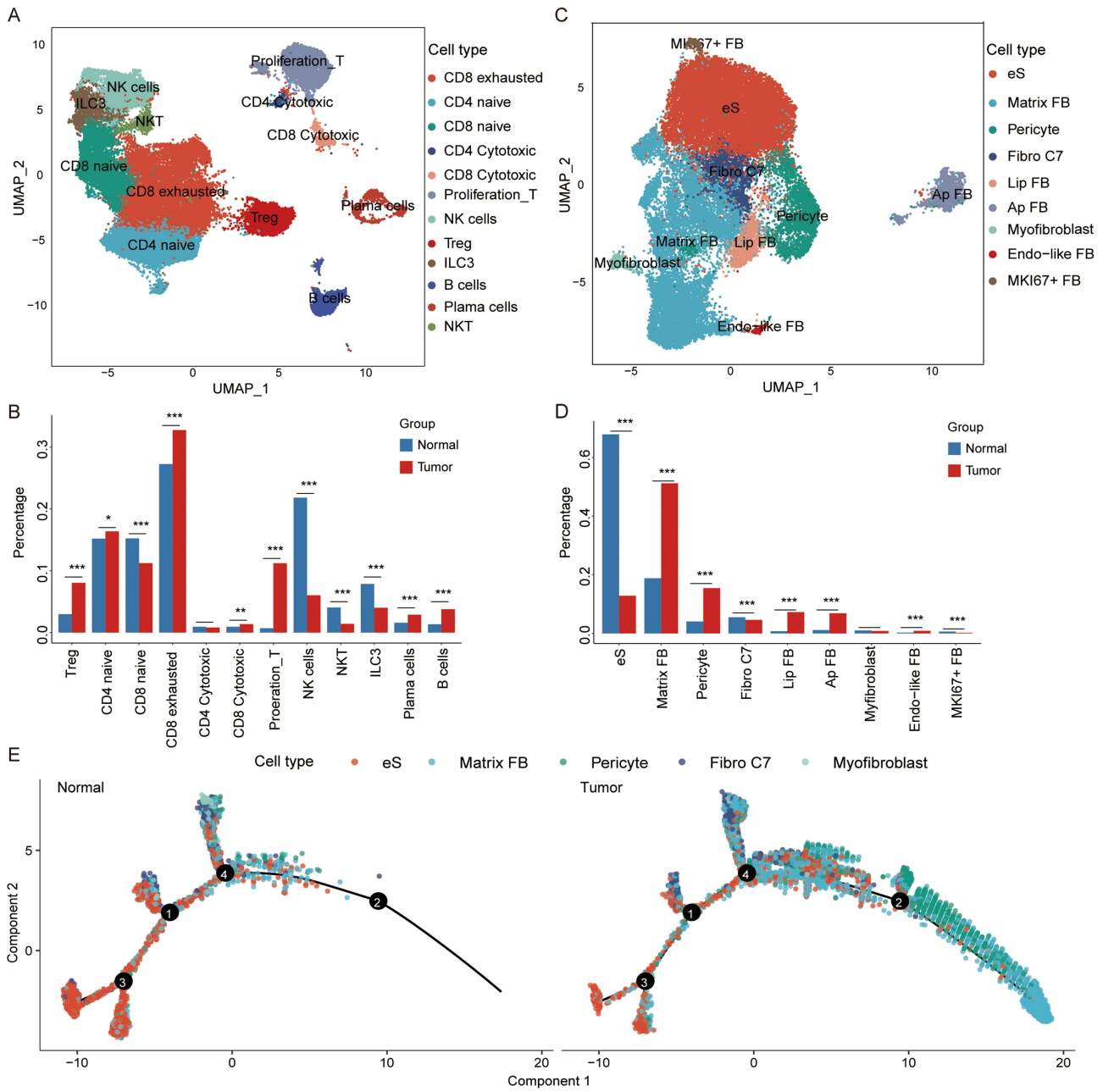

Figure 6 Examined the cell population landscapes of lymphocytes and stromal fibroblasts in the endometrial microenvironment. (**A**) The UMAP projection revealed lymphocytes divided into 12 subtypes. (**B**) Significantly changed the proportion of lymphocytes in the normal and tumor groups. (**C**) UMAP projection revealed stromal fibroblasts divided into nine subtypes. (**D**) Significantly changed the proportion of stromal fibroblasts in the normal and tumor groups. (**E**) Pseudotime analysis revealed different subtypes forming a relative developmental trajectory of stromal fibroblasts. Levels of significance were defined as $*p < 0.05$, $**p < 0.01$, and $***p < 0.001$.

annotation stage and differentiation trajectory, this study concentrated on myeloid cells in the immune microenvironment to offer fresh insights. M2_like2 macrophages were identified as terminally differentiated cells, with their proportion significantly heightened in the tumor microenvironment. CNVs and gene enrichment analysis suggested a potential pro-cancer role for these cells, leading to their inclusion in the cell communication analysis. Matrix FBs within the stromal fibroblast population exhibited notable changes in the cell evolutionary trajectory, representing the largest proportion of stromal fibroblasts in tumor tissues and significantly increased compared to the normal group. Consequently, this cluster was also included in the cell communication analysis.

https://doi.org/10.2147/IJWH.S530666

In this study, we utilized the R package CellChat to conduct a systematic cell communication analysis focusing on SOX9+LGR5-, SOX9+LGR5+, M2_like2, M2_like1, and Matrix FBs, with a specific emphasis on receptor-ligand interactions. Initially, we visualized the overall interaction between the cell groups. Subsequently, through chord plots and heatmaps, we displayed the level of interaction between different cell groups. Figure 7A illustrated a lower number of cell communications in the Tumor group, with higher intensity, indicating an intriguing phenomenon. Our primary focus was on the strength of cell-to-cell communication, revealing that SOX9+LGR5- cells and M2_like2 in the Tumor group engaged in particularly strong communication (Figure 7B), suggesting their critical role in the tumor microenvironment. Similar conclusions were drawn from the cell-receiving and cell-signaling graphs (Figure 7C). The tumor group exhibited a robust outgoing interaction strength of SOX9+LGR5- and Matrix FB, along with a potent incoming interaction strength of M2_like2 (Figure 7C, Appendix Figure 6A and B), indicating a heightened level of communication between malignant epithelial cells and the entire microenvironment in endometrial cancer development.

By progressively narrowing down our focus to the most intense communication, we centered on M2_like2 and SOX9+LGR5- cells. Further ligand analysis unveiled that these cells generated robust signals through MIF-(CD74+CD44) interactions (Figure 7D and Appendix Figure 6C). Immunofluorescence co-localization revealed that MIF is co-expressed with the epithelial cell marker E-cadherin in EC tissues, suggesting a high level of MIF expression in EC epithelial cells (Figure 7E). In our previous study, we identified the highly active transcription factor NFKB2 in the SOX9+LGR5- cell subset through SCENIC analysis. Additionally, GSEA analysis on the NFKB2 transcription factor indicated a significant enhancement of its activity in endometrial cancer. Notably, our investigation revealed that NFKB2 regulates the target gene CD44, which was highlighted in bold in Appendix Table 6. We hypothesized the interaction between MIF and CD44 was mediated by NFKB2. There appeared to be robust crosstalk between the M2_like2 and SOX9+LGR5- cells, where the highly active transcription factor NFKB2 in the SOX9+LGR5- cells modulates CD44 by interacting with MIF on the M2_like2 cells. To explore whether NFKB2 mediates MIF's regulation of CD44 in epithelial cells, we conducted cell-based experiments. We first evaluated NFKB2 and CD44 protein expression across five EC cell lines, finding that CD44 was highly expressed in RL95-2 and KLE cells but lower in Ishikawa, HEC-1a, and AN3CA cells. Conversely, NFKB2 levels were low in Ishikawa cells and higher in the other four lines (Figure 7F and Appendix Figure 7A). We then observed that recombinant human MIF (rhMIF) enhanced NFKB2 and CD44 expression in Ishikawa cells (Figure 7G and Appendix Figure 7B). siRNA knockdown of NFKB2 reduced rhMIF-induced CD44 upregulation (Figure 7H and Appendix Figure 7C–E).

Gene Expression and Survival Analysis

TCGA Data Analysis observed that the mRNA expression levels of MIF and NFKB2 in endometrial cancer tissues were significantly higher than those in the Normal group, whereas the opposite was true for CD44 (Figure 8A). Furthermore, single-cell sequencing data revealed substantially increased expression levels of MIF, NFKB2, and CD44 in endometrial cancer compared to the normal group (Figure 8B).

By analyzing publicly available endometrial cancer data from TCGA (https://cancergenome.nih.gov/), we delved into the clinical significance of these genes. Survival analysis unveiled a significant statistical variance in patient survival time between high and low CD44 expression levels. These findings underscored that high expression of CD44 served as a negative prognostic indicator for EC patients (Figure 8C). Combining NFKB2 and CD44 into a gene panel, where high expression of either gene denoted high expression, our study demonstrated that this gene panel also correlated with unfavorable survival outcomes (Appendix Figure 7F).

Discussion

The tumor microenvironment comprises various components that intricately interact to propel the malignant transformation and progression of endometrial epithelial cells. Single-cell transcriptome analysis has emerged as a pivotal tool for exploring the tumor microenvironment, unraveling its multidimensional intricacies, and delving into the pathogenesis, diagnosis, and treatment of tumors. In this study, we conducted a comprehensive integration analysis of publicly available scRNA-seq data on EC, aiming to restructure the microenvironment at a single-cell resolution. In addition to insights gleaned from existing literature on single-cell analysis of EC, this study also referenced markers linked to normal

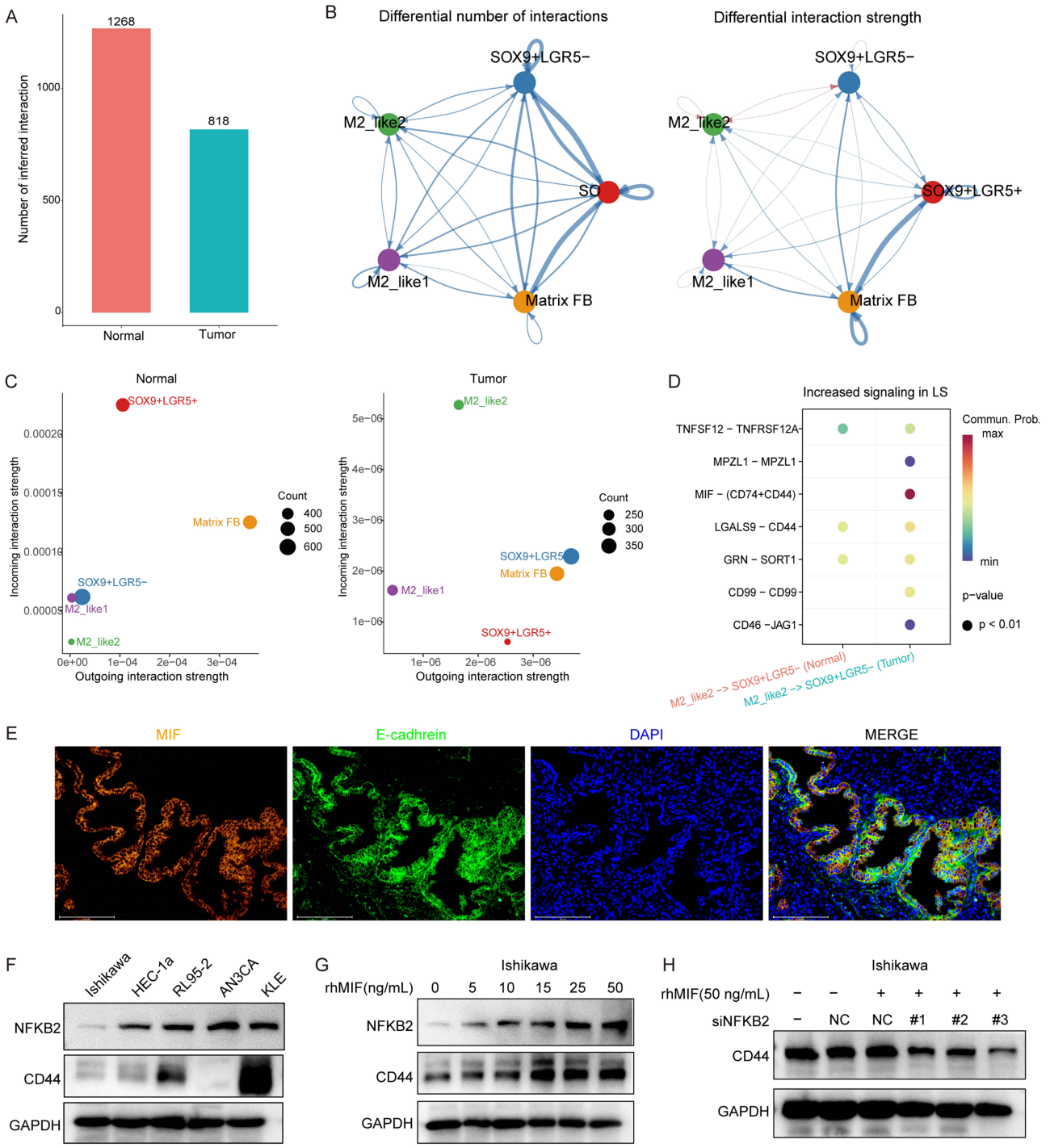

Figure 7 Cell Communication in the Endometrial Microenvironment and Experimental Validation (**A**) Bar plots indicated fewer cell communications in the Tumor group, with a higher intensity of cell communication. (**B**) NetVisual chord plots illustrated strong communication between SOX9+LGR5- cells and M2_like2 in the Tumor group. (**C**) Cell-receiving and cell-signaling plots displayed the strong outgoing interaction strength of SOX9+LGR5- and Matrix FB, and the strong incoming interaction strength of M2_like2. (**D**) Receptor-ligand plots showed strong interactions between M2_like2 and SOX9+LGR5- mediated by the ligand-receptor pair MIF-(CD74+CD44) expression of MIF, NFKB2, and CD44. (**E**) Immunofluorescence co-localization revealed that MIF was co-expressed with the epithelial cell marker E-cadherin in EC tissues. (**F**) NFKB2 levels were low in Ishikawa cells and higher in the other four lines. (**G**) rhMIF enhanced NFKB2 and CD44 expression in Ishikawa cells. (**H**) siRNA knockdown of NFKB2 reduced rhMIF-induced CD44 upregulation. -: indicated the absence of rhMIF treatment; +: indicated the presence of rhMIF treatment; NC: negative control siRNA; #1, #2, #3: represented three different siRNA sequences targeting NFKB2.

https://doi.org/10.2147/IJWH.S530666

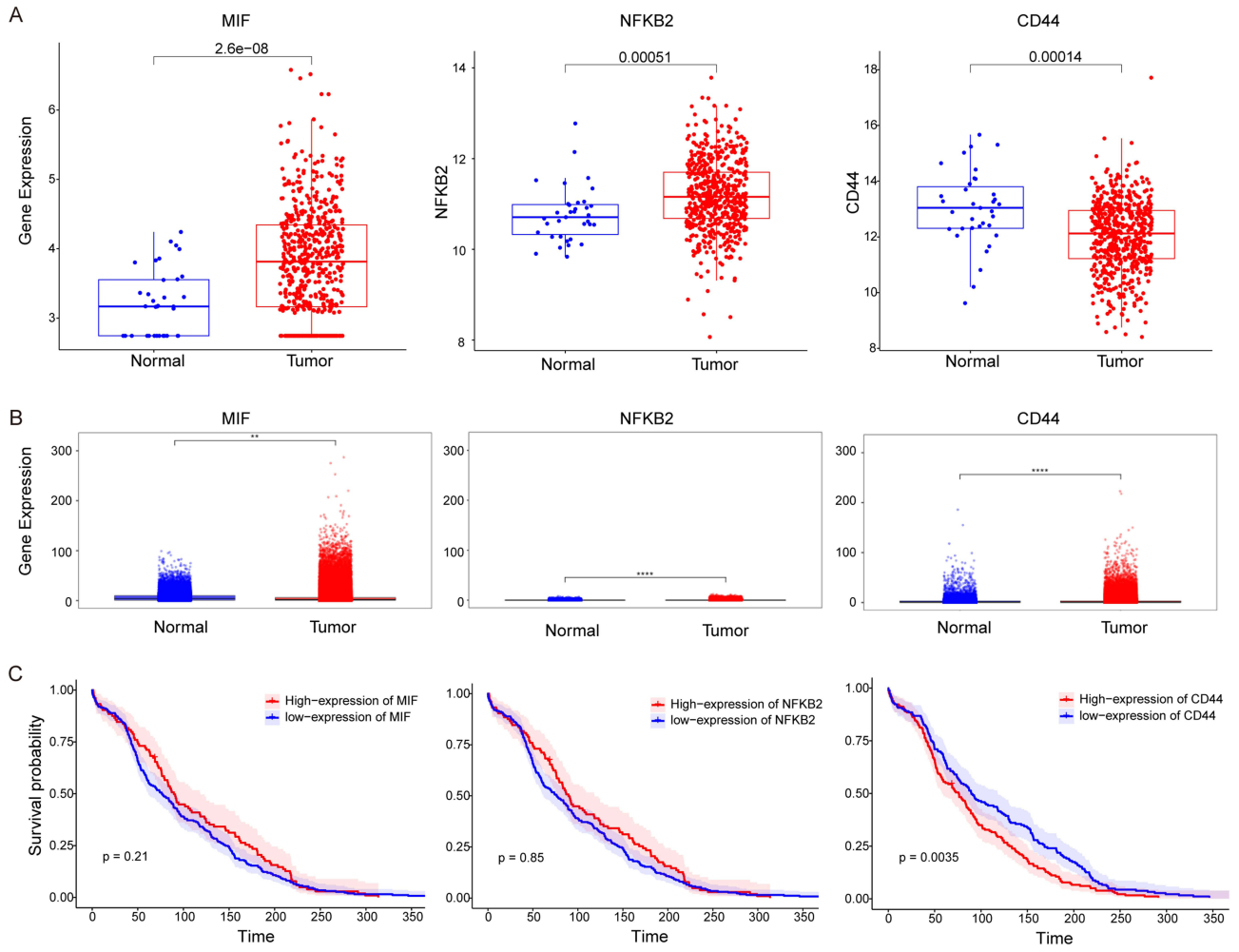

Figure 8 Gene Expression and Survival Analysis. (**A**) mRNA expression levels of MIF, NFKB2, and CD44 in EC tissues. (**B**) mRNA expression levels of MIF, NFKB2, and CD44 of single-cell sequencing data in EC tissues were significantly higher than those in the normal group. (**C**) Survival analysis revealed differences in patient survival time between high and low mRNA expression levels of MIF, NFKB2, and CD44. Levels of significance were defined as *$p < 0.05$, **$p < 0.01$, and ***$p < 0.001$.

menstrual cycles and other markers specific to endometrial cells.[27–30] Consequently, we provided detailed annotations of subtypes within epithelial cells, macrophages, lymphocytes, and stromal fibroblasts.

In this study, we consulted multiple studies on the endometrium and furnished detailed annotations of epithelial cells, encompassing the SOX9+ cell types (SOX9+LGR5- and SOX9+LGR5+), glandular secretory epithelial cells, and ciliated epithelial cells. This study serves as the comprehensive report on epithelial cell annotations in EC research. Our study unveiled that the menstrual cycle in EC deviated from normal conditions, leading to the manifestation of characteristics of both glandular secretory epithelial cells and ciliated epithelial cells in SOX9+ cell types. In essence, these cells transitioned from glandular secretory epithelial cells.

Guo et al[5] postulated that stem cell-like epithelial cells differentiate into glandular secretory epithelial cells, which subsequently transform into ciliated cells. Another study[8] suggested that glandular secretory non-ciliated epithelial cells act as the source of EC and progress through carcinogenic subgroups to evolve into ciliated epithelial cells. Our research complemented the findings of these studies. Specifically, SOX9+LGR5- represented a cluster of aggressively proliferative epithelial cells with a high expression of the SOX9 gene, originating from glandular secretory epithelial cells. According to the inferred copy number results, SOX9+LGR5- exhibited a higher degree of malignancy, while SOX9+LGR5+ also demonstrated copy number alterations. These findings align with existing literature, indicating a significant correlation between SOX9+LGR5+ or SOX9+LGR5- cells and poor prognosis in EC.[30]

A prior study identified LCN2+/SAA1/2+ cells as a distinct subgroup associated with endometrial tumor development.[8,31] In our study, NMF analysis of malignant epithelial cells unveiled six programs, with the feature genes of program four encompassing LCN2, SAA1, and SAA2. This implies that the NMF algorithm may serve as a suitable tool for uncovering biological processes, effectively simplifying large and complex matrices into a few interpretable gene programs. This methodology proves particularly useful for highly heterogeneous tumor cells, with potential for further in-depth exploration in the future.[32]

This study corroborated the previous findings, illustrating the phenomenon of macrophage polarization from M1 to M2. Macrophages adhered to the continuum activation model. However, our research indicated that M_remodeling cells represented the terminal differentiation state, potentially influencing extracellular matrix remodeling.[33] Functional enrichment analysis pinpointed M2_like2 cells as the predominant subset of macrophages, actively engaging in NFKB signaling pathways. M2-like2 subtype exhibited high activity of transcription factors such as CEBPA, STAT1, IRF9, MXI1, and MAX. CEBPA likely plays a role in promoting the activation and maturation of M2-like macrophages, leading to the production and release of cytokines and molecules involved in interacting with the tumor microenvironment. STAT1, as a signaling transducer, may be associated with anti-tumor immunity. IRF9 is an interferon regulatory factor involved in regulating the interferon signaling pathway. MXI1 and MAX are both MYC-interacting proteins, and their activation may contribute to tumor development by activating the MYC pathway. These findings shed light on the gene regulatory networks that support Myeloid plasticity by identifying key TFs responsible for regulating or maintaining the gene expression programs within the identified Myeloid subtypes.

Cell communication analysis suggested that M2_like2 cells exert varying degrees of influence on non-immune cells, underscoring their pivotal role in the tumor immune microenvironment. Through the evolution of macrophages, functional enrichment analysis, and the heightened expression of specific marker genes, the M2_like2 cells delineated in this study likely corresponded to the same cluster as the C1QC+ macrophages mentioned in Guo et al's research.

Beyond published research, this study identified a cell cluster, M2_like1, characterized by elevated expression of TNF and MAF genes.[33] Within the Tumor group, this subtype transitioned into M_remodeling alongside M2_like2 in the terminal phase of macrophage differentiation. Given the inefficient initiation of monocytes in trajectory differentiation within the Tumor group, yet their swift differentiation into two M2 subtypes at the culmination of differentiation, it appears to represent an adaptive response to M2 polarization, further evolving into M_remodeling. Further investigation is warranted to comprehend the functional significance of this rapid transition in EC. Guo's study noted that activated macrophage populations exhibited low expression of IL-1B, indicating their anti-inflammatory characteristics. Building on these insights, steering macrophage transcriptomes toward the M1 phenotype could emerge as a potential therapeutic avenue for EC. Our study reached similar conclusions, suggesting that impeding macrophages from polarizing into M2 and M_remodeling subtypes, or promoting the differentiation of more monocytes into M1 macrophages, could constitute promising anti-cancer strategies.

Macrophage Migration Inhibitory Factor (MIF) serves as a versatile protein with dual roles as a pro-inflammatory cytokine and a chemotactic factor, regulating the expression of other pro-inflammatory factors.[34,35] MIF promotes the expression of α(v)β(3) integrin and vascular endothelial growth factor in EC cells.[36] Besides, knocking down MIF in vitro can suppress the proliferation and migration of EC cells.[36,37] Notably, a recent publication in study highlighted MIF as a key drug resistance factor in EC.[38] Targeting MIF could prove pivotal in combating the onset and drug resistance mechanisms of EC. CD44, a gene associated with tumor metastasis, belongs to the cell adhesion molecule family[39] and serves as a marker for tumor stem cells. Dysregulated CD44 expression has been observed across various cancers such as ovarian, breast, pancreatic, gastric, and colorectal cancers. The level of CD44 expression closely correlates with tumor proliferation capacity, differentiation status, and patient prognosis. A previous study indicated that NF-κB regulates CD44 expression, impacting the proliferation and invasiveness of breast cancer cells.[40,41] Our findings suggest that communication between the M2_like2 macrophage cluster and the SOX9+LGR5- cell cluster within TAMs of EC may be mediated through the MIF-(CD74+CD44) signaling axis. Transcriptional regulatory analysis indicates that this interaction may be controlled by the transcription factor NFKB2. Further immunofluorescence co-localization revealed that MIF was co-expressed with the epithelial cell marker E-cadherin in EC tissues. In vitro, MIF stimulation enhances the expression of NFKB2 and CD44 proteins in EC epithelial cells, while NFKB2 knockdown

inhibits MIF-induced CD44 expression. An important consideration arising from our survival analysis was that while high expression of CD44 was significantly associated with poor patient prognosis, a similar correlation was not observed for its upstream regulators MIF and NFKB2 at the bulk transcriptomic level. This apparent discrepancy highlighted the intricate nature of tumor biology and can be interpreted through several lenses. First, the biological functions of MIF and NFKB2 are primarily dictated by post-translational modifications and protein activity, not just mRNA abundance. Second, our single-cell data revealed that this signaling axis was specific to the interaction between M2_like2 macrophages and SOX9+LGR5- epithelial cells; this context-specific effect was likely diluted and masked in bulk tissue analyses. Finally, CD44 acts as a downstream convergence point for multiple oncogenic pathways, making its expression a more robust, integrated marker of tumor progression.

Our investigation into lymphocytes corroborated existing research, revealing a notable increase in Treg cells in EC.[8] In a study by Chen et al, there was only a trend towards increased CD4 naive, CD8 exhausted, and B cells in EC; however, our research identified statistically significant differences, underscoring the advantage of a larger sample size in enhancing research robustness. Moreover, a study found that specific tumor-infiltrating lymphocyte subtypes correlated with improved overall survival. Interestingly, our results indicated a contrasting role for Treg cells, aligning with findings from a previous study. Notably, FOXP3+ CD4 Treg lymphocytes associated with immune suppression were notably enriched in EC samples, hinting at potential immune evasion mechanisms in EC. Ligand-receptor pairs like CD74-MIF, CD74-COPA, and CD74-APP may facilitate interactions between cytotoxic CD8 cells, Treg cells, and other cells, suggesting avenues for further exploration into the communications between SOX9+LGR5- and M2-like2 cells in cellular escape mechanisms.

Our study delved into the evolutionary trajectory of stromal fibroblasts, where activated stromal fibroblasts differentiated into myofibroblasts and pericytes. Myofibroblasts play a crucial role in tissue repair by producing collagen in response to damage.[42] However, prolonged activation can lead to excessive collagen deposition, scar formation, or fibrosis, as seen in EC studies. Other research focused on the crosstalk between stromal fibroblasts and malignant epithelial cells, categorizing fibroblasts into mCAF, iCAF, vCAF, and apCAF subtypes.[6] The vCAFs, termed pericytes in our study, were associated with aggressive EC progression and poor prognosis, exhibiting high expression of RGS5 and GJA4, in line with findings from Ren et al's article.[8,43] The previous article also noted that this cluster differentiated relatively late, and our study suggested that pericytes may continue to differentiate into terminal fibroblasts through the PFT process. Targeting the "pericyte-fibroblast transition" process could offer novel therapeutic avenues for preventing and treating EC metastasis.[44] While the proportion of CAFs decreased in EC samples, studies have indicated their role in enhancing endometrial epithelial cell proliferation. Our findings suggest that the Normal group may harbor a higher proportion of quiescent stromal fibroblasts, while the Tumor group exhibits a shift towards activated stromal fibroblasts. The late-stage differentiation process of PFT may remodel the extracellular matrix and support malignant cell growth.

The primary strength of this study lied in its comprehensive, integrated analysis of multiple single-cell datasets, which allowed for a detailed annotation of the EC microenvironment. Critically, we moved beyond computational prediction by providing experimental validation for the key identified MIF-NFKB2-CD44 signaling axis. We acknowledged, however, certain limitations and nuances. For instance, while high CD44 expression was prognostic in bulk survival data, its upstream regulators MIF and NFKB2 were not. This highlighted a broader limitation of retrospective data and underscores that many of our other findings remain predictive. Therefore, future work is essential to validate these interactions and explore their therapeutic potential. A key clinical application lies in refining patient selection for Fertility-Sparing Treatment, where understanding the tumor's "molecular fingerprint" is paramount for success.[45] Our work contributed to this goal by identifying potential biomarkers for better risk stratification. Furthermore, future therapeutic strategies targeting this axis could be complemented by considering the role of metabolic health and nutraceuticals, such as inositols and alpha-lipoic acid, which are gaining attention in gynecological oncology.[46]

In conclusion, our study unveiled a detailed transcriptomic landscape of human EC, shedding light on the EC microenvironment and emphasizing the significant communication between the M2_like2 macrophage subpopulation and the SOX9+LGR5- epithelial cell subpopulation. NFKB2 was identified as a mediator of MIF activity through the CD44 receptor in EC, providing deeper insights into cancer initiation and progression.

Data Sharing Statement

The datasets generated and/or analysed during the current study are available in the SRA database (accession number PRJNA650549), NCBI SRA database under the accession number SRP349751, and the Gene Expression Omnibus (accession number GSE173682).

Ethics Statement

This study was based on publicly available data. The requirement for ethical approval was waived by the Institutional Review Board of the First Affiliated Hospital of Xiamen University, as the data were de-identified and publicly accessible.

Author Contributions

All authors made a significant contribution to the work reported, whether that is in the conception, study design, execution, acquisition of data, analysis and interpretation, or in all these areas; took part in drafting, revising or critically reviewing the article; gave final approval of the version to be published; have agreed on the journal to which the article has been submitted; and agree to be accountable for all aspects of the work.

Funding

This work was supported by the National Natural Science Foundation of China (No. 82271678), the Natural Science Foundation of Fujian Province (No. 2022J02058 and No. 2023J01623).

Disclosure

The authors report no conflicts of interest in this work.

References

1. Xia C, Dong X, Li H, et al. Cancer statistics in China and United States, 2022: profiles, trends, and determinants. *Chin Med J*. 2022;135(5):584–590. doi:10.1097/CM9.0000000000002108
2. Klemm F, Joyce JA. Microenvironmental regulation of therapeutic response in cancer. *Trends Cell Biol*. 2015;25(4):198–213. doi:10.1016/j.tcb.2014.11.006
3. Sahoo SS, Zhang XD, Hondermarck H, et al. The emerging role of the microenvironment in endometrial cancer. *Cancers*. 2018;10(11):408. doi:10.3390/cancers10110408
4. Ren X, Kang B, Zhang Z. Understanding tumor ecosystems by single-cell sequencing: promises and limitations. *Genome Biol*. 2018;19(1):211. doi:10.1186/s13059-018-1593-z
5. Guo YE, Li Y, Cai B, et al. Phenotyping of immune and endometrial epithelial cells in endometrial carcinomas revealed by single-cell RNA sequencing. *Aging*. 2021;13(5):6565–6591. doi:10.18632/aging.202288
6. Yu Z, Zhang J, Zhang Q, et al. Single-cell sequencing reveals the heterogeneity and intratumoral crosstalk in human endometrial cancer. *Cell Prolif*. 2022;55(6):e13249. doi:10.1111/cpr.13249
7. Horeweg N, Workel HH, Loiero D, et al. Tertiary lymphoid structures critical for prognosis in endometrial cancer patients. *Nat Commun*. 2022;13(1):1373. doi:10.1038/s41467-022-29040-x
8. Ren X, Liang J, Zhang Y, et al. Single-cell transcriptomic analysis highlights origin and pathological process of human endometrioid endometrial carcinoma. *Nat Commun*. 2022;13(1):6300. doi:10.1038/s41467-022-33982-7
9. Chen J, Song Y, Huang J, et al. Integrated single-cell RNA sequencing and spatial transcriptomics analysis reveals the tumour microenvironment in patients with endometrial cancer responding to anti-PD-1 treatment. *Clin Transl Med*. 2024;14(4):e1668. doi:10.1002/ctm2.1668
10. Regner MJ, Wisniewska K, Garcia-Recio S, et al. A multi-omic single-cell landscape of human gynecologic malignancies. *Mol Cell*. 2021;81(23):4924–4941. doi:10.1016/j.molcel.2021.10.013
11. Zheng GX, Terry JM, Belgrader P, et al. Massively parallel digital transcriptional profiling of single cells. *Nat Commun*. 2017;8:14049. doi:10.1038/ncomms14049
12. Hao Y, Hao S, Andersen-Nissen E, et al. Integrated analysis of multimodal single-cell data. *Cell*. 2021;184(13):3573–3587. doi:10.1016/j.cell.2021.04.048
13. Sun S, Zhu J, Ma Y, et al. Accuracy, robustness and scalability of dimensionality reduction methods for single-cell RNA-seq analysis. *Genome Biol*. 2019;20(1):269. doi:10.1186/s13059-019-1898-6
14. Becht E, McInnes L, Healy J, et al. Dimensionality reduction for visualizing single-cell data using UMAP. *Nat Biotechnol*. 2018. doi:10.1038/nbt.4314
15. Korsunsky I, Millard N, Fan J, et al. Fast, sensitive and accurate integration of single-cell data with Harmony. *Nat Methods*. 2019;16(12):1289–1296. doi:10.1038/s41592-019-0619-0
16. Kanehisa M, Goto S. KEGG: kyoto encyclopedia of genes and genomes. *Nucleic Acids Res*. 2000;28(1):27–30. doi:10.1093/nar/28.1.27

17. Yu G, Wang LG, Han Y, et al. clusterProfiler: an R package for comparing biological themes among gene clusters. *OMICS*. 2012;16(5):284–287. doi:10.1089/omi.2011.0118
18. Mootha VK, Lindgren CM, Eriksson KF, et al. PGC-1alpha-responsive genes involved in oxidative phosphorylation are coordinately down-regulated in human diabetes. *Nat Genet*. 2003;34(3):267–273. doi:10.1038/ng1180
19. Deng C, Deng G, Chu H, et al. Construction of a hypoxia-immune-related prognostic panel based on integrated single-cell and bulk RNA sequencing analyses in gastric cancer. *Front Immunol*. 2023;14:1140328. doi:10.3389/fimmu.2023.1140328
20. Puram SV, Tirosh I, Parikh AS, et al. Single-cell transcriptomic analysis of primary and metastatic tumor ecosystems in head and neck cancer. *Cell*. 2017;171(7):1611–1624. doi:10.1016/j.cell.2017.10.044
21. Qiu X, Mao Q, Tang Y, et al. Reversed graph embedding resolves complex single-cell trajectories. *Nat Methods*. 2017;14(10):979–982. doi:10.1038/nmeth.4402
22. La Manno G, Soldatov R, Zeisel A, et al. RNA velocity of single cells. *Nature*. 2018;560(7719):494–498. doi:10.1038/s41586-018-0414-6
23. Aibar S, González-Blas CB, Moerman T, et al. SCENIC: single-cell regulatory network inference and clustering. *Nat Methods*. 2017;14 (11):1083–1086. doi:10.1038/nmeth.4463
24. Jin S, Guerrero-Juarez CF, Zhang L, et al. Inference and analysis of cell-cell communication using CellChat. *Nat Commun*. 2021;12(1):1088. doi:10.1038/s41467-021-21246-9
25. Colaprico A, Silva TC, Olsen C, et al. TCGAbiolinks: an R/Bioconductor package for integrative analysis of TCGA data. *Nucleic Acids Res*. 2016;44(8):e71. doi:10.1093/nar/gkv1507
26. Yang M, Jiang H, Ding X, et al. Multi-omics integration highlights the role of ubiquitination in endometriosis fibrosis. *J Transl Med*. 2024;22 (1):445. doi:10.1186/s12967-024-05245-0
27. Chen T, Xu Y, Xu X, et al. Comprehensive transcriptional atlas of human adenomyosis deciphered by the integration of single-cell RNA-sequencing and spatial transcriptomics. *Protein Cell*. 2024;15(7):530–546. doi:10.1093/procel/pwae012
28. Fonseca M, Haro M, Wright KN, et al. Single-cell transcriptomic analysis of endometriosis. *Nat Genet*. 2023;55(2):255–267. doi:10.1038/s41588-022-01254-1
29. Garcia-Alonso L, Handfield LF, Roberts K, et al. Mapping the temporal and spatial dynamics of the human endometrium in vivo and in vitro. *Nat Genet*. 2021;53(12):1698–1711. doi:10.1038/s41588-021-00972-2
30. Wang W, Vilella F, Alama P, et al. Single-cell transcriptomic atlas of the human endometrium during the menstrual cycle. *Nat Med*. 2020;26 (10):1644–1653. doi:10.1038/s41591-020-1040-z
31. Takehara M, Sato Y, Kimura T, et al. Cancer-associated adipocytes promote pancreatic cancer progression through SAA1 expression. *Cancer Sci*. 2020;111(8):2883–2894. doi:10.1111/cas.14527
32. Barkley D, Moncada R, Pour M, et al. Cancer cell states recur across tumor types and form specific interactions with the tumor microenvironment. *Nat Genet*. 2022;54(8):1192–1201. doi:10.1038/s41588-022-01141-9
33. Li Y, Ren P, Dawson A, et al. Single-cell transcriptome analysis reveals dynamic cell populations and differential gene expression patterns in control and aneurysmal human aortic tissue. *Circulation*. 2020;142(14):1374–1388. doi:10.1161/CIRCULATIONAHA.120.046528
34. Osipyan A, Chen D, Dekker FJ. Epigenetic regulation in macrophage migration inhibitory factor (MIF)-mediated signaling in cancer and inflammation. *Drug Discov Today*. 2021;26(7):1728–1734. doi:10.1016/j.drudis.2021.03.012
35. Liang J, Lei K, Liang R, et al. Single-cell RNA sequencing reveals the MIF-ACKR3 receptor-ligand interaction between iCAFs and tumor cells in esophageal squamous cell carcinoma. *Cell Signal*. 2024;117:111093. doi:10.1016/j.cellsig.2024.111093
36. Bondza PK, Metz CN, Akoum A. Macrophage migration inhibitory factor up-regulates alpha(v)beta(3) integrin and vascular endothelial growth factor expression in endometrial adenocarcinoma cell line Ishikawa. *J Reprod Immunol*. 2008;77(2):142–151. doi:10.1016/j.jri.2007.07.004
37. Md FA, Omar SZ, Mohamed Z, et al. High throughput silencing identifies novel genes in endometrioid endometrial cancer. *Taiwan J Obstet Gynecol*. 2018;57(2):217–226. doi:10.1016/j.tjog.2018.02.009
38. Hu Z, Wu Z, Liu W, et al. Proteogenomic insights into early-onset endometrioid endometrial carcinoma: predictors for fertility-sparing therapy response. *Nat Genet*. 2024;56(4):637–651. doi:10.1038/s41588-024-01703-z
39. Hassn MM, Syafruddin SE, Mohtar MA, et al. CD44: a Multifunctional Mediator of Cancer Progression. *Biomolecules*. 2021;11(12). doi:10.3390/biom11121850
40. Smith SM, Lyu YL, Cai L. NF-κB affects proliferation and invasiveness of breast cancer cells by regulating CD44 expression. *PLoS One*. 2014;9 (9):e106966. doi:10.1371/journal.pone.0106966
41. Jiang P, Tian C, Zheng Y, et al. The prognostic value of co-expression of stemness markers CD44 and CD133 in endometrial cancer. *Front Oncol*. 2024;14:1338908. doi:10.3389/fonc.2024.1338908
42. Younesi FS, Miller AE, Barker TH, et al. Fibroblast and myofibroblast activation in normal tissue repair and fibrosis. *Nat Rev Mol Cell Biol*. 2024. doi:10.1038/s41580-024-00716-0
43. Lu G, Du R, Liu Y, et al. RGS5 as a biomarker of pericytes, involvement in vascular remodeling and pulmonary arterial hypertension. *Vasc Health Risk Manag*. 2023;19:673–688. doi:10.2147/VHRM.S429535
44. Hosaka K, Yang Y, Seki T, et al. Pericyte-fibroblast transition promotes tumor growth and metastasis. *Proc Natl Acad Sci U S A*. 2016;113(38): E5618–E5627. doi:10.1073/pnas.1608384113
45. De Paola L, Napoletano G, Gullo G, et al. The era of increasing cancer survivorship: trends in fertility preservation, medico-legal implications, and ethical challenges. *Open Med*. 2025;20(1):20251144. doi:10.1515/med-2025-1144
46. Laganà AS, Monti N, Fedeli V, et al. Does alpha-lipoic acid improve effects on polycystic ovary syndrome? *Eur Rev Med Pharmacol Sci*. 2022;26 (4):1241–1247. doi:10.26355/eurrev_202202_28116